Supporting Information

Probing the free energy landscape of the fast folding gpW protein by relaxation dispersion NMR

Celia Sanchez-Medina, Ashok Sekhar, Pramodh Vallurupalli, Michele Cerminara, Victor Muñoz and Lewis E. Kay

Supporting Methods

Free Energy Surface Model and Analysis of T-jump Kinetics

The free energy surface model that we use for the analysis of the infrared temperature-jump data has been described in detail before[1,2]. In general, it is a mean-field model that generates a one-dimensional free energy surface (FES) according to a single order parameter termed nativeness (*n*) that is assumed to operate as a good reaction coordinate for folding. The order parameter nativeness is defined as the probability of finding any given residue in the native dihedral angles (the specific sets of dihedral angles that are found in the native 3D structure). Therefore it is a local order parameter that goes from 0 for the fully unfolded state (all residues in non-native angles) to 1 for the native structure (all residues in native angles). Using this definition it is straightforward to define a relation that determines the changes in conformational entropy of the protein as a function of nativeness[2]:

$$\Delta S_{conf}(n) = N\left(-R\left[n\ln(n)+(1-n)\ln(1-n)\right]+(1-n)\Delta S_{conf,res}\right) \qquad [S1]$$

where n is nativeness, $\Delta S_{conf,res}$ is the average cost in conformational entropy of fixing one residue with native angles and N is the number of residues in the protein. The function that determines the changes in stabilization enthalpy (energy from interactions different from solvation free energy) as a function of nativeness is taken to be a Markov chain, which is equivalent to assume that native interactions are broken at a constant rate as the protein becomes increasingly disordered. Particularly, the stabilization enthalpy functional is defined as

$$\Delta H(n) = N\Delta H_{res}\left[\left(1-x^{(1-n)}\right)/(1-x)\right] \qquad [S2]$$

where ΔH_{res} is the total stabilization energy per residue, and the parameter x determines the rate of change of the stabilization energy as a function of n. Thus, the decay in stabilization enthalpy as the protein moves away from the fully native state ($n=1$) is exponential, and the term within square brackets in Eq. S2 is the fraction of the enthalpy present at any given value of nativeness. The protein specific parameter x determines how sharply the stabilization enthalpy decays; x is determined by the structural class and the specifics of the protein native structure and sequence[2]. Here we have directly used Eq. S2 with ΔH_{res} and x as adjustable

parameters to fit the experimental laser-induced temperature-jump data (rates and amplitudes).

The change in heat capacity as a function of the order parameter is treated in a similar way, and defined by the following expression

$$\Delta C_p(n) = \Delta C_{p,res}\left[\left(1-x_c^{(1-n)}\right)/(1-x_c\right] \qquad \text{[S3]}$$

where $\Delta C_{p,res}$ is the change in heat capacity per residue and x_c the characteristic rate of change of the heat capacity as a function of n. Combining Eqs. S1-S3 we obtain the free energy surface as a function of the order parameter

$$\Delta G(n) = \Delta H(n) - T\Delta S(n) + \Delta C_p(n)\left[(T-T_m) + T\ln(T/385)\right] \qquad \text{[S4]}$$

where T_m is the denaturation midpoint temperature (temperature at which the protein is half unfolded) for the protein and 385 K is the convergence temperature for the folding entropy[1]. Eq. S4 can be used directly to calculate the FES of a protein as a function of temperature from which the probability distribution can be obtained.

The relaxation kinetics are calculated as simple diffusion on the FES assuming a diffusion coefficient (D) that is constant as function of the nativeness parameter n, but depends on the solvent viscosity and temperature according to the following expression

$$D = \frac{k_0}{\eta(T)}\exp(-NE_a/RT) \qquad \text{[S5]}$$

where η is the viscosity of water as a function of temperature, k_o is the pre-factor and E_a is the activation energy per residue. Note that in this model, the temperature dependence of the relaxation rateis determined by D(equation S5) and from any changes in the FES shape induced by temperature as defined in equation S4.

For all the calculations described in this work we use a fixed value of $\Delta S_{conf,res}$ =16.5 J/(mol.K), which we generated by calculating the average value obtained from the Robertson and Murphy analysis of a database of calorimetric data [3]. For additional simplicity we fixed $\Delta C_{p,res}$ to the average value of 53.5 (52.5 J/(mol.K) obtained empirically by Robertson and Murphy[3]) and x_c to 0.0136, that has been used before by us[1]. We thus fit the infrared laser induced temperature-jump kinetic data (relaxation rate and amplitude as a function of temperature) to a model of four parameters (ΔH_{res}, x, k_0 and E_a), using N=61 for gpW. The overall parameters obtained from the fit to the gpW data at pH 3.5 are: ΔH_{res} = 4.23 kJ/mol, x=0.94, k_0=1.37x10^{12} s^{-1} and E_a =0.877 kJ/mol.

References

(1) Naganathan, A. N.; Doshi, U.; Muñoz, V. *J. Am. Chem. Soc.* **2007**, *129*, 5673-5682.

(2) De Sancho, D.; Muñoz, V. *Phys. Chem. Chem. Phys.* **2011**, *13*, 17030-17043.

(3) Robertson, A. D.; Murphy, K. P. *Chem. Rev.* **1997**, *97*, 1251-1268.

(4) Shen, Y.; Delaglio, F.; Cornilescu, G.; Bax, A. *J. Biomol. NMR* **2009**, *44*, 213-223.

(5) Tamiola, K.; Acar, B.; Mulder, F. A. *J. Am. Chem. Soc.* **2010**, *132*, 18000-18003.

(6) Skrynnikov, N. R.; Dahlquist, F. W.; Kay, L. E. *J. Am. Chem. Soc.* **2002**, *124*, 12352-12360.

(7) Orekhov, V. Y.; Korzhnev, D. M.; Kay, L. E. *J. Am. Chem. Soc.* **2004**, *126*, 1886-1891.

(8) Bouvignies, G.; Korzhnev, D. M.; Neudecker, P.; Hansen, D. F.; Cordes, M. H.; Kay, L. E. *J. Biomol. NMR* **2010**, *47*, 135-141.

(9) Lundström, P.; Teilum, K.; Carstensen, T.; Bezsonova, I.; Wiesner, S.; Hansen, D. F.; Religa, T. L.; Akke, M.; Kay, L. E. *J. Biomol. NMR* **2007**, *38*, 199-212.

(10) Vallurupalli, P.; Bouvignies, G.; Kay, L. E. *J. Phys. Chem. B* **2011**, *115*, 14891-14900.

(11) Hansen, D. F.; Vallurupalli, P.; Lundström, P.; Neudecker, P.; Kay, L. E. *J. Am. Chem. Soc.* **2008**, *130*, 2667-2675.

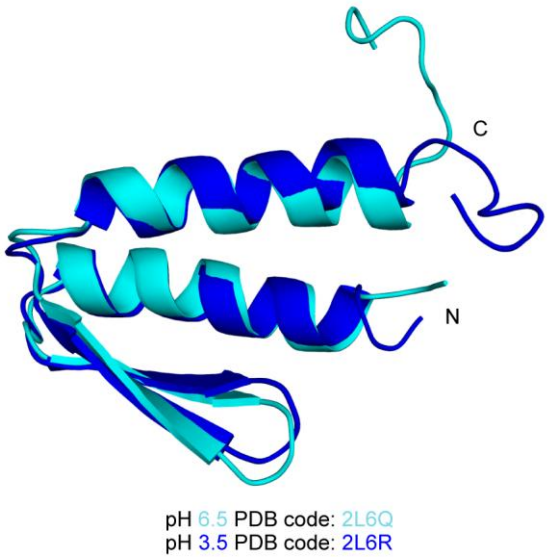

Figure S1. Superposition of NMR derived structures of gpW at pH 3.5 (blue, PDB: 2L6R), and at pH 6.5 (cyan, PDB: 2L6Q). Structures were superimposed using backbone heavy atoms (excluding CO).

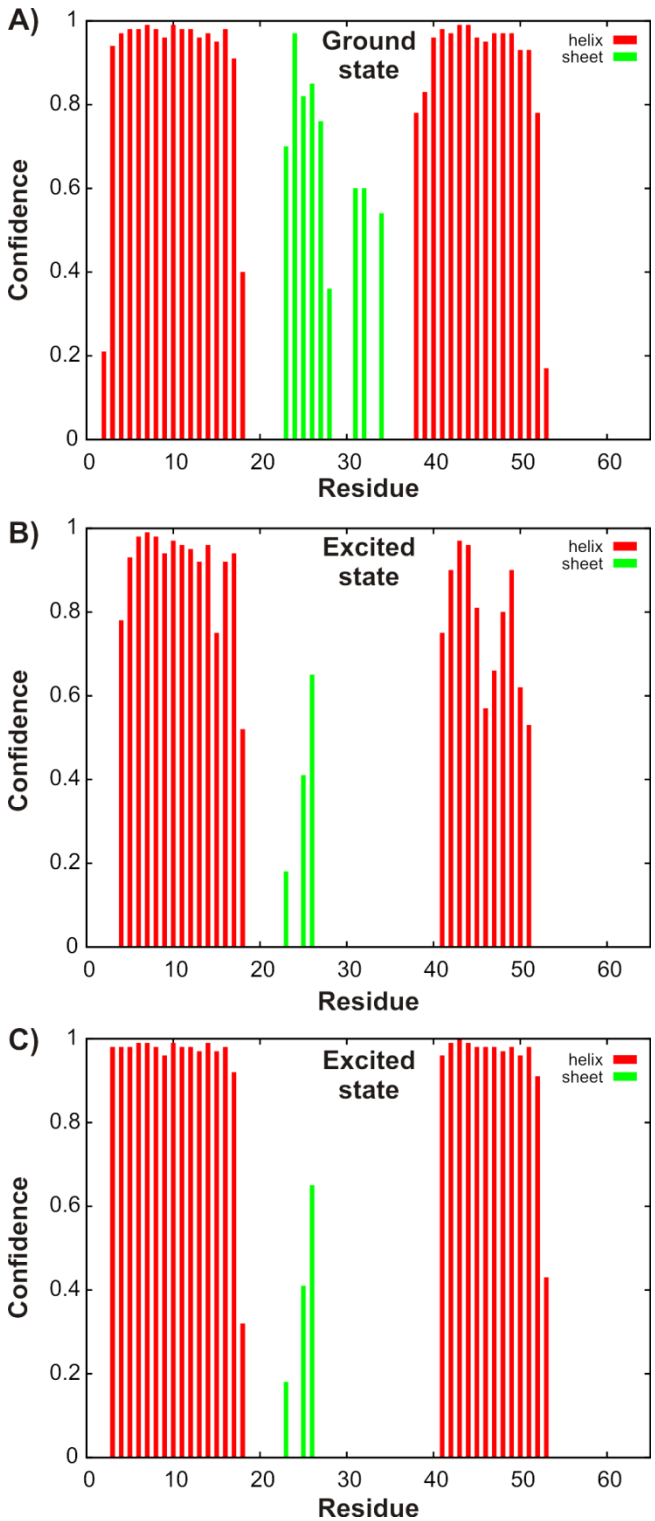

Figure S2. Confidence of secondary structural elements of state *X*, as predicted by TALOS+ [4]. A) Predicted secondary structure of the native state. B) Predicted secondary structure for the excited state. For residues localized to helices in the native gpW conformation and where signs of $\Delta\varpi_{XN} = \varpi_X - \varpi_N$ could not be determined experimentally, they were chosen so as to position ϖ_X closer to the random coil chemical shift. C) As in B but with the signs of $\Delta\varpi_{XN}$ chosen such that ϖ_X is placed further from the random coil chemical shift. Where the signs

were not available for nuclei in the beta hairpin in the native conformation, they were chosen so as to move ϖ_X closer to the random coil chemical shift (in both B and C).

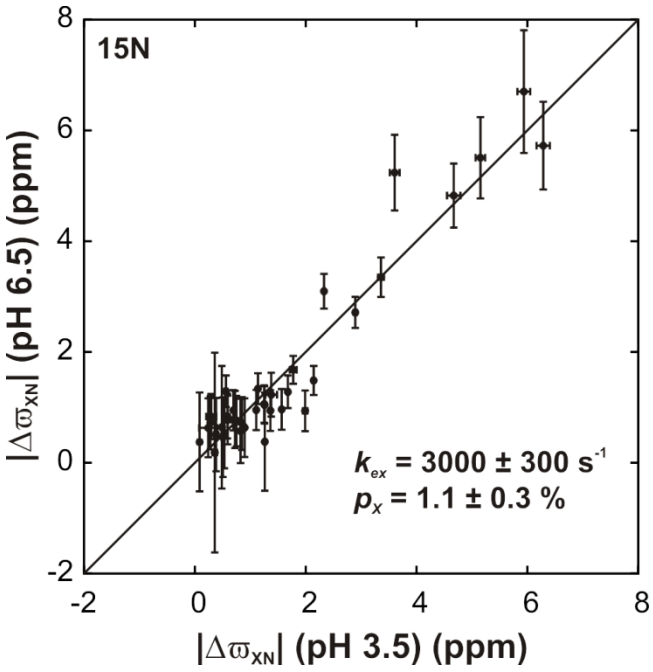

Figure S3. The excited state observed for gpW at pH 3.5 is also present at pH 6.5. Correlation between $|\Delta\varpi_{XN}|$ values for backbone ^{15}N nuclei, pH 3.5,*vs*those obtained at pH 6.5. Chemical shift differences at pH 6.5 were extracted from fits of ^{15}N RD profiles recorded at 11.7 T on a sample of ^{15}N-labeled gpW dissolved in a buffer comprised of 25 mM sodium phosphate, 50 mM NaCl, 0.5 mM EDTA, 0.5 mM NaN_3/10% D_2O, pH 6.5. Dispersion profiles were fit to a two-state model to extract p_X, k_{ex} and $\Delta\varpi_{XN}$ values. Although these values may not be accurately determined at pH 6.5 because of the availability of data at only a single static magnetic field, the clear correlation obtained between $|\Delta\varpi_{XN}|$ at pH 3.5 and 6.5 establishes that very similar excited states are present at the two pH values.

Table S1

^{15}N and $^{1}H^{N}$ chemical shifts for the native state, ϖ_N, and differences in chemical shifts between excited and native states $\Delta\varpi_{XN} = \varpi_X - \varpi_N$ of the gpW protein, 1°C.

Res	ϖ_N (ppm) $^{15}N^a$	ϖ_N (ppm) $^{1}H^{N\,a}$	ϖ_{RC} (ppm) $^{15}N^b$	ϖ_{RC} (ppm) $^{1}H^{N\,b}$	$\Delta\varpi_{XN}$ (ppm) $^{15}N^c$	$\Delta\varpi_{XN}$ (ppm) $^{1}H^{Nc}$
M1	-	-	-	-	-	-
V2	122.49	8.78	121.75	8.20	0.49 ± 0.02	0.000 ± 0.032
R3	124.88	8.95	125.71	8.47	0.75 ± 0.02	-0.096 ± 0.002
Q4	118.61	8.76	122.03	8.49	-1.26 ± 0.01	0.000 ± 0.289
E5	120.04	7.89	122.37	8.52	+0.29 ± 0.09	0.253 ± 0.005
E6	121.70	8.34	121.60	8.39	0.00 ± 1.00	0.000 ± 0.095
L7	121.77	8.42	123.10	8.21	-0.35 ± 0.05	0.069 ± 0.006
A8	121.51	7.93	124.74	8.21	+0.59 ± 0.07	-0.133 ± 0.003
A9	121.03	8.17	123.26	8.19	0.82 ± 0.01	0.000 ± 0.114
A10	d	d	123.20	8.21	d	d
R11	117.33	8.53	120.64	8.26	+0.90 ± 0.02	-0.153 ± 0.003
A12	123.92	8.08	125.81	8.35	-0.38 ± 0.04	0.000 ± 0.097
A13	121.88	7.90	122.87	8.16	0.00 ± 0.61	-0.196 ± 0.003
L14	d	d	121.01	8.04	d	d
H15	117.22	8.06	119.39	8.41	0.51 ± 0.02	-0.116 ± 0.003
D16	121.42	8.49	121.57	8.27	-1.11 ± 0.02	-0.124 ± 0.002
L17	120.33	7.97	122.41	8.10	+1.14 ± 0.02	-0.186 ± 0.002
M18	117.39	8.31	120.91	8.36	0.53 ± 0.03	0.000 ± 0.190
T19	108.70	7.53	115.43	8.25	+1.68 ± 0.02	-0.224 ± 0.002
G20	107.59	7.58	111.53	8.46	+2.90 ± 0.03	+0.343 ± 0.003
K21	121.30	8.03	121.29	8.18	-0.56 ± 0.03	-0.142 ± 0.002
R22	120.78	8.73	122.55	8.35	+1.99 ± 0.04	-0.391 ± 0.003
V23	e	e	122.31	8.23	e	e
A24	127.29	8.81	128.49	8.46	+1.57 ± 0.02	-0.276 ± 0.002
T25	115.83	8.61	113.34	8.08	-1.26 ± 0.02	-0.347± 0.002
V26	119.96	8.90	123.00	8.23	+3.61 ± 0.09	-0.604 ± 0.010
Q27	122.79	8.61	124.80	8.46	2.33 ± 0.01	0.032 ± 0.008
K28	127.76	9.13	122.68	8.44	-4.67 ± 0.12	-0.462 ± 0.005
D29	e	e	121.52	8.39	e	e
G30	103.89	8.72	109.40	8.35	+5.15 ± 0.09	-0.334 ± 0.003
R31	119.73	7.74	121.22	8.19	0.85 ± 0.02	0.304 ± 0.003
R32	122.43	8.57	123.15	8.43	-0.41 ± 0.02	0.015 ± 0.014
V33	127.72	9.02	122.21	8.27	5.27 ± 0.21	0.701 ± 0.023
E34	d	d	124.79	8.43	d	d
F35	122.66	9.19	121.44	8.32	1.94 ± 0.20	0.990 ± 0.039
T36	110.45	8.22	116.26	8.07	+5.94 ± 0.12	-0.059 ± 0.007
A37	121.97	9.22	126.66	8.41	4.67 ± 0.27	0.763 ± 0.031
T38	107.25	7.92	113.33	8.13	+6.29 ± 0.12	-0.264 ± 0.003
S39	115.94	8.14	118.57	8.37	+3.36 ± 0.05	+0.233 ± 0.003
V40	122.95	e	122.65	8.27	1.63 ± 0.39	e
S41	116.43	9.06	120.07	8.47	-1.38 ± 0.10	-0.739 ± 0.007
D42	121.91	7.75	122.11	8.36	0.00 ± 0.88	+0.593 ± 0.007
L43	124.86	7.74	122.62	8.12	-1.77 ± 0.06	+0.588 ± 0.011

K44	118.86	8.53	122.26	8.27	+0.36 ± 0.04	-0.132 ± 0.004
K45	120.84	7.88	122.28	8.30	-0.21 ± 0.07	-0.032 ± 0.010
Y46	122.27	7.75	121.37	8.13	+0.24 ± 0.16	0.375 ± 0.003
I47	119.32	8.34	123.24	7.86	+1.36 ± 0.02	0.176 ± 0.005
A48	119.78	7.80	128.01	8.39	+2.15 ± 0.03	-0.108 ± 0.003
E49	d	d	119.73	8.31	d	d
L50	120.74	8.20	123.00	8.25	-0.76 ± 0.02	0.000 ± 0.112
E51	118.58	8.23	121.56	8.36	-0.69 ± 0.02	0.000 ± 0.170
V52	119.40	7.54	121.54	8.20	0.72 ± 0.02	-0.191 ± 0.002
Q53	121.72	8.28	124.81	8.56	0.59 ± 0.02	0.047 ± 0.007
T54	112.59	8.15	115.72	8.27	+1.25 ± 0.02	0.097 ± 0.003
G55	110.42	8.18	111.32	8.45	0.28 ± 0.05	0.133 ± 0.003
M56	119.93	8.19	120.08	8.25	0.01 ± 0.71	0.028 ± 0.005
T57	115.50	8.21	115.34	8.24	0.00 ± 0.43	0.040 ± 0.008
Q58	d	d	122.84	8.43	d	d
R59	d	d	122.92	8.42	d	d
R60	123.61	8.56	123.13	8.44	0.05 ± 0.09	0.000 ± 0.021
R61	123.80	8.61	123.20	8.48	0.09 ± 0.05	0.000 ± 0.010
G62	115.51	8.29	-	-	0.18 ± 0.03	0.000 ± 0.032

[a] ^{15}N and ^{1}H^{N} chemical shifts in the native state (ϖ_N) were measured from an ^{1}H^{N}-^{15}N HSQC spectrum recorded at 1 ºC.

[b] Random coil (RC) values, ϖ_{RC}, were predicted using the Neighbor Corrected Intrinsically Disordered Protein Library[5].

[c] Values of $\Delta\varpi$ have been measured by RD NMR experiments, as described in the text. Where possible, signs of $\Delta\varpi_{XN}$ (^{15}N) have been obtained by a comparison of peak positions in (i) sets of HSQC and HMQC experiments recorded at 11.7 T and 18.8T and/or in (ii) pairs of HSQC experiments measured at 11.7, 18.8T, as described previously [6].Signs could not be obtained for those shift values that do not have + or -. Signs of ^{1}H^{N} $\Delta\varpi_{XN}$ values were determined on the basis of (i) ^{1}H^{N}/^{15}N zero-quantum and double-quantum coherence relaxation dispersion experiments[7] or (ii) from a comparison of peak positions in the directly detected dimension of HSQC experiments acquired at 11.7 T and 18.8 T [8].

[d] Overlapped peaks.

[e] Peaks do not appear in spectra.

Table S2

$^{13}C^{O}$ and $^{13}C^{\alpha}$ chemical shifts for the native state, ϖ_N, of the gpW protein and differences in shifts between excited and native states $\Delta\varpi_{XN} = \varpi_X - \varpi_N$, 1°C.

Res	ϖ_N (ppm) $^{13}C^{O}$ [a]	ϖ_N (ppm) $^{13}C^{\alpha}$ [b]	ϖ_{RC} (ppm) $^{13}C^{O}$ [c]	ϖ_{RC} (ppm) $^{13}C^{\alpha}$ [c]	$\Delta\varpi_{XN}$ (ppm) $^{13}C^{O}$ [d]	$\Delta\varpi_{XN}$ (ppm) $^{13}C^{\alpha}$ [e]
M1	172.27	f	-	-	-0.39 ± 0.01	f
V2	176.53	62.81	176.03	62.12	-0.60 ± 0.01	g
R3	177.36	58.76	176.07	56.07	-0.61 ± 0.02	0.75 ± 0.05
Q4	178.12	59.31	175.76	55.80	-0.76 ± 0.02	0.77 ± 0.03
E5	178.56	58.57	176.47	56.70	-0.93 ± 0.01	0.66 ± 0.03
E6	178.68	h	176.48	56.64	-1.00 ± 0.01	h
L7	177.15	57.82	177.19	55.24	0.57 ± 0.01	g
A8	180.62	f	177.49	52.49	-0.77 ± 0.01	f
A9	f	54.78	177.67	52.57	f	0.25 ± 0.04
A10	178.73	f	177.86	52.50	0.50 ± 0.03	f
R11	179.22	60.28	176.07	56.06	-0.77 ± 0.01	0.88 ± 0.05
A12	178.79	f	177.36	52.44	0.33 ± 0.02	f
A13	f	54.92	177.87	52.58	f	0.53 ± 0.02
L14	177.35	58.00	177.43	55.17	0.25 ± 0.03	g
H15	177.29	59.38	174.38	55.95	-1.02 ± 0.02	1.02 ± 0.03
D16	177.40	57.22	176.13	54.22	0.95 ± 0.03	1.15 ± 0.04
L17	180.01	57.29	177.83	55.49	-0.97 ± 0.02	g
M18	177.34	f	176.51	55.55	-0.45 ± 0.03	f
T19	174.59	61.20	175.00	61.95	+0.31 ± 0.12	0.85 ± 0.02
G20	174.83	h	173.98	45.24	-1.38 ± 0.01	h
K21	176.29	56.26	176.60	56.15	0.70 ± 0.05	0.60 ± 0.03
R22	f	57.96	176.04	56.07		2.29 ± 0.11
V23	172.91	59.81	175.71	62.19	+2.58 ± 0.03	g
A24	175.25	51.44	177.89	52.55	+2.12 ± 0.02	0.93 ± 0.02
T25	173.69	h	174.53	61.87	+0.49 ± 0.18	h
V26	173.39	59.74	176.09	62.39	+2.13 ± 0.02	g
Q27	174.79	f	175.79	55.77	+1.38 ± 0.12	f
K28	f	55.75	176.22	56.44	h	1.42 ± 0.05
D29	175.19	55.07	176.87	54.53	0.80 ± 0.09	1.48 ± 0.04
G30	173.15	h	174.06	45.27	+0.63 ± 0.01	h
R31	173.60	54.10	176.20	55.83	+2.03 ± 0.02	2.07 ± 0.10
R32	h	f	175.91	55.90	h	f
V33	f	61.58	176.02	62.30	f	h
E34	175.00	f	176.04	56.48	0.04 ± 4.08 [i]	f
F35	f	57.41	176.01	57.98	f	0.28 ± 0.04
T36	h	j	173.63	61.58	h	j
A37	h	55.50	177.96	52.62	h	2.72 ± 0.07
T38	175.08	63.62	174.71	61.94	1.34 ± 0.03	1.30 ± 0.02
S39	h	j	174.44	58.28	h	j
V40	176.85	66.56	176.16	62.35	+0.45 ± 0.15	g
S41	176.90	61.92	174.18	58.33	-0.72 ± 0.08	1.30 ± 0.04
D42	178.14	56.97	176.25	54.30	0.53 ± 0.17	0.90 ± 0.03
L43	177.59	57.49	177.58	55.41	0.55 ± 0.02	g

K44	179.20	60.83	176.59	56.35	-0.72 ± 0.01	0.93 ± 0.03
K45	177.73	59.62	176.26	56.46	-0.57 ± 0.02	0.83 ± 0.02
Y46	176.46	58.66	175.61	57.83	0.29 ± 0.05	0.95 ± 0.03
I47	176.48	66.19	175.45	60.82	0.10 ± 0.18	g
A48	f	54.64	177.87	52.44	f	0.41 ± 0.03
E49	178.72	58.58	176.58	56.63	-1.05 ± 0.01	0.84 ± 0.04
L50	179.20	57.07	177.50	55.36	0.66 ± 0.01	g
E51	177.46	58.33	176.35	56.52	0.50 ± 0.02	0.81 ± 0.05
V52	177.56	64.64	176.19	62.42	0.66 ± 0.01	g
Q53	176.76	57.15	175.98	55.79	0.22 ± 0.02	0.40 ± 0.04
T54	f	62.70	174.97	62.05	f	0.26 ± 0.04
G55	173.97	45.57	174.23	45.32	0.06 ± 0.05	0.00 ± 0.06
M56	176.28	55.91	176.63	55.47	0.00 ± 0.50	0.04 ± 0.18
T57	f	62.24	174.45	61.86	f	0.19 ± 0.03
Q58	f	55.70	175.75	55.73	f	0.11 ± 0.07
R59	175.73	f	176.04	55.95	0.13 ± 0.02	f
R60	175.67	56.14	175.95	55.86	0.12 ± 0.02	0.20 ± 0.02
R61	175.47	f	176.57	56.12	0.00 ± 0.05	f
G62	-	h	-	-	-	h

[a] $^{13}C^{O}$chemical shifts were measured from 2D ($^{13}C^{O}$,$^{1}H^{N}$) HNCO-based spectra recorded on a U-^{15}N/^{13}C gpW sample, 1^{o}C.

[b]$^{13}C^{\alpha}$ shifts were measured on a U-^{15}N and ^{13}C-selectively labeled sample (using 2-^{13}C-glucose as the ^{13}C source[9]).

[c]ϖ_{RC} values were predicted using the Neighbor Corrected Intrinsically Disordered Protein Library[5].

[d]$\Delta\varpi_{XN}$ values were obtained by fitting $^{13}C^{O}$RD CPMG profiles using fixed values for k_{ex} (4087 ± 42 s^{-1}) and p_X (9.0 ± 0.3 %), that, in turn, were generated by simultaneous fits of ^{15}N, $^{1}H^{N}$ and ^{13}C-methyl RD curves and the static magnetic field dependence of ^{15}N chemical shifts as described in the text [10]. Signs of $\Delta\varpi_{XN}$ values were obtained from peak positions in $^{1}H^{N}$-$^{13}C^{O}$correlation maps where the $^{13}C^{O}$ chemical shift was recorded either as single quantum or multiple quantum (^{15}N-$^{13}C^{O}$or$^{1}H^{N}$-$^{13}C^{O}$) coherence[11]. Experiments were recorded at 11.7 and 18.8T.

[e]$^{13}C^{\alpha}$ shift differences were obtained by fitting RD CPMG profiles using fixed values for k_{ex} (4087 ± 42 s^{-1}) and p_X (9.0 ± 0.3 %), as described above. Dispersion profiles derived from I or V were not included because the $^{13}C^{\alpha}$ spins are not isolated ($^{13}C^{\beta}$ labeling) while L is not labeled at the C-α position using 2-^{13}C-glucose as the ^{13}C source[9]. Signs of $\Delta\varpi_{XN}$ values could not be obtained because of the limited quality of $^{1}H^{\alpha}$ – $^{13}C^{\alpha}$ correlation maps.

[f] Overlapped peaks.

[g] I,L,V residues that cannot be quantified.

[h] Very weak peak or does not appear in the spectra.

[i] Not used in analysis

[j] Peak is overlapped with the water signal

Table S3

^{13}C-methyl chemical shifts for the native state of the gpW protein, ϖ_N ,and chemical shift differences between the excited and native states $\Delta\varpi_{XN} = \varpi_X - \varpi_N$, 1^{o}C.

Residue Number[a]	ϖ_N (ppm) ^{13}C[b]	$\Delta\varpi_{XN}$ (ppm) ^{13}C[c]
M1ε	16.887	0.07 ± 0.06
V2γa	20.517	d
V2γb	e	e
L7δa	24.054	0.56 ± 0.01
L7δb	e	e
A8β	e	e
A9β	18.165	0.16 ± 0.03
A10β	18.615	0.30 ± 0.02
A12β	e	e
A13β	e	e
L14δa	23.940	0.69 ± 0.01
L14δb	e	e
L17δa	22.152	1.78 ± 0.02
L17δb	26.283	1.14 ± 0.02
M18ε	16.342	0.32 ± 0.01
V23γa	20.483	0.85 ± 0.00
V23γb	20.607	0.00 ± 0.04
A24β	23.099	f
V26γa	21.157	0.00 ± 0.16
V26γb	22.059	1.09 ± 0.01
V33γa	21.461	0.18 ± 0.05
V33γb	21.775	1.31 ± 0.01
A37β	18.496	0.56 ± 0.01
V40γa	e	e
V40γb	23.664	1.11 ± 0.01
L43δa	21.276	2.52 ± 0.09
L43δb	26.096	1.94 ± 0.08
A48β	18.117	0.19 ± 0.03
L50δa	22.168	0.71 ± 0.01
L50δb	25.059	0.00 ± 0.14
V52γa	21.241	0.00 ± 0.06
V52γb	21.672	0.40 ± 0.03
M56ε	16.818	0.09 ± 0.05

[a] The letters a and b next to the atom labels refer to upfield (a) or downfield (b) peaks as they appear in the ^{13}C dimension.

[b] Native state $^{13}CH_3$ chemical shifts were obtained from a ^{1}H-^{13}C correlation map recorded at 1ºC.

[c] Chemical shift differences for the methyl group were obtained by fitting RD CPMG profiles acquired at 11.7 and 18.8 T, 1ºC, as described in the text.

[d] The peak shows coupling.

[e] Overlapped peaks

[f] Peak is either very weak, does not appear in the spectrum or it is impossible to get a reliable $\Delta\varpi$ value.

[g] Only some atoms of Leu, Val, Ala and Met sidechains have been used in the analysis, in accordance with the labeling scheme expected from growth with 1-^{13}C-glucose as the carbon source [9].